A simple material model for composite based on elements with realistic stiffness

T. Tryland

SINTEF Manufacturing, Raufoss, Norway

1 Background

The obvious question is how to combine models and data to create a virtual prediction tool? There is a long history with measured data to adjust finite element models representing the geometry and material properties of a tested component. It seems to be a good starting point to represent the initial geometry with correct stiffness and challenge the element formulations to maintain realistic stiffness even when the elements are severely deformed. A proper discretisation is crucial when building a finite element model, and most metallic parts are represented as continuums although we know about the elementary particles. It is likely that this simplification is acceptable as long as the strains are small and the strain hardening is sufficient to compensate for local variation in material properties, but remember that brittle behaviour may be the result when the elastic energy stored in the component is allocated into the first local area that fails. It may therefore be an idea to include local variations in the material properties [1], and the result may be smaller elements than required to describe the geometry. One example here is 3D-printed components that may have reduced ductility due to local variation in the material properties above a critical limit [2].

Figure 1 illustrates the pultrusion process that is similar to an extrusion process to make different cross-sections, but in addition comes the rovings to add stiffness along the profile and different fabric mats to add stiffness in other directions as well [3]. There is a need for a design tool to optimise both the profile geometry and the orientations of the fibres inside it to secure sufficient stiffness and strength to withstand every relevant loading situation. Note that the fibres under tension contributes effectively to the strength. However, support from the matrix material is required to keep eventual fibres under compression in position and thereby utilise their strength. It is therefore likely that a profile in composite material based on fibres and matrix will show higher stiffness and strength in tension compared with in compression. Figure 1 also show the profile example that is planned with continuous mats both at the outer and inner surfaces as well as in the middle to have a sufficient fraction of the fibres oriented ±45° relative to the profile length. This profile was used as base for this study where the main objective was to find an engineering approach with scaled fibres and resin as a design tool for composite structures.

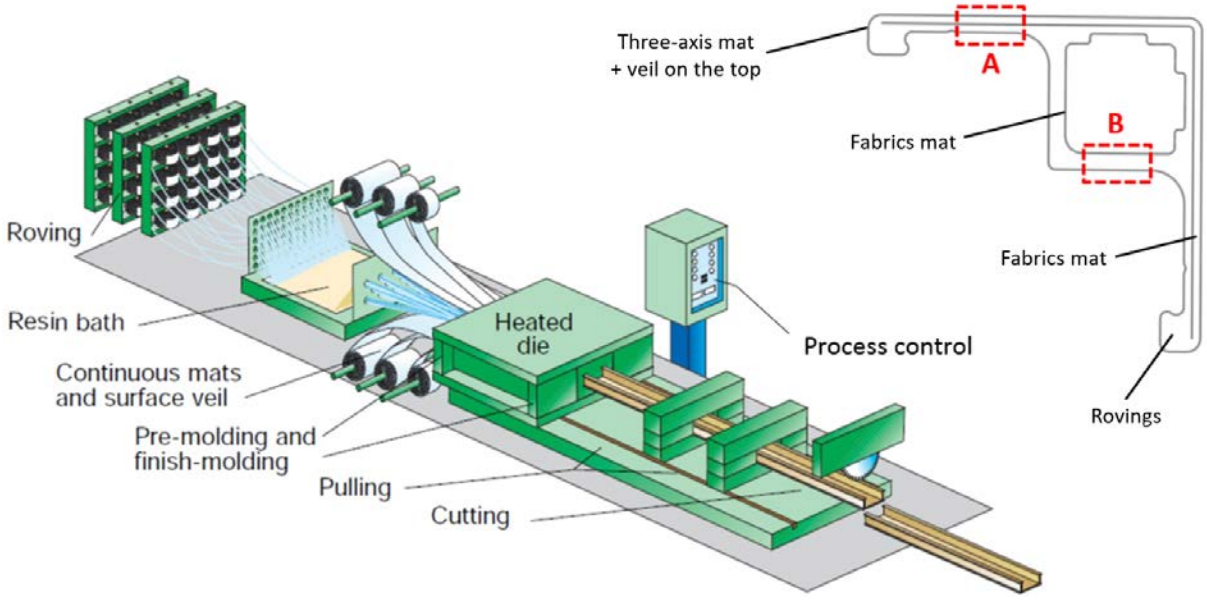

Fig.1: The process is flexible with respect to cross-section and fibre layout to strengthen it.

2 Scaling of fibres and matrix

It is a challenge to measure for example the stiffness and strength of a specimen cut from the composite profile shown in figure 1. Here it is important to notice the difference between specimens cut from positions A and B. The first one has surface mats on both sides as well as fabrics in the middle, while the second one means a non-symmetric specimen with different surface mats on the two sides. It is also worth to remember that cutting test specimens from the profile cross-section may reduce the stiffness and strength contribution from fibres without anchoring at their free ends. Does it make sense to measure average properties when the component is far from uniform?

Figure 2 illustrates some examples with scaling of fibres and matrix in the different layers through the wall thickness of a pultruded profile. Note that the two illustrations at left hand side show the same case with and without matrix to display the far too thick fibres in the middle as well as in the surface layers. It is also worth to notice the element mesh that was made by a final split to obtain hexahedrons close to cubes geometrically of pentahedron elements to obtain common nodes between elements representing longitudinal fibres, fibres oriented ±45° as well as elements representing the matrix in between the fibres. The behaviour of the through-thickness-cubes was simulated under compression where all nodes at the upper and lower surface was fixed. This means buckling length like half the thickness for the longitudinal fibres, and the capacity under compression was meet when the matrix around struggle to keep the fibres in position. Note that the fibres at right hand side are far too thick and thereby able to utilise their strength, while the refined variant at right hand side has thinner fibres that require more support from the matrix around them. There is no challenges with proper connection between different materials in the numerical model, and the distance between the fibres and the shear stiffness of the matrix relative to the glass fibres seems to be the most important parameters.

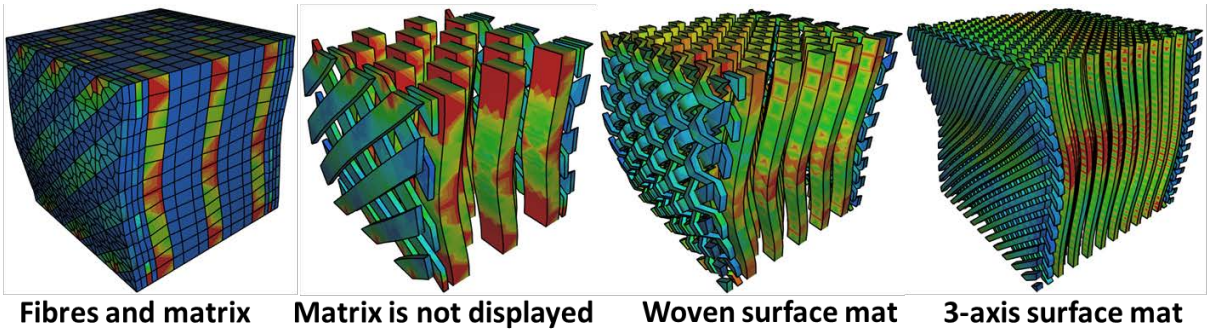

Fig.2: Some examples illustrating scaling of fibres and matrix for a through-thickness cube.

In reality, it may be a challenge to secure proper connection between fibres and matrix, and the fibres are far too thin to be represented without some scaling. However, it seems like even the coarse models in figure 2 capture the physical phenomena that limits the stiffness and strength of a composite. The results show that the fibres in the surface mats does not contribute effectively to stiffness and strength in this case with axial compression, but they are required to secure some robustness and stiffness in the other directions as well. It is also worth to notice that woven mats seems to be even more flexible than 3-axis mats with more straight fibres. However, there is no fibres in the thickness direction, and delamination between different layers through the thickness is therefore the likely result under compression. This also explains why the fibre- and matrix material strengths times their fraction of the profile cross-section may be a reasonable estimate for the tensile strength, while the compressive strength is lower than this for many profile geometries.

3 Specimen geometry, test procedure and numerical simulations of the tests

Experiments were therefore run on the profile level with axial compression to challenge the stiffness of the matrix material. Figure 3 defines both the complete profile and the corner part only with tests at different lengths to evaluate the effect of both cross-section slenderness and global stiffness. Note that cutting the free flanges means two local areas along the profile without the surface mat and reduced stiffness and strength contribution from fibres without anchoring at their free ends. The profile ends were examined in a light microscope looking for initial failures, and none of the tested specimens had visible cracks inside the cross-section like the most severe one shown at right hand side in figure 3.

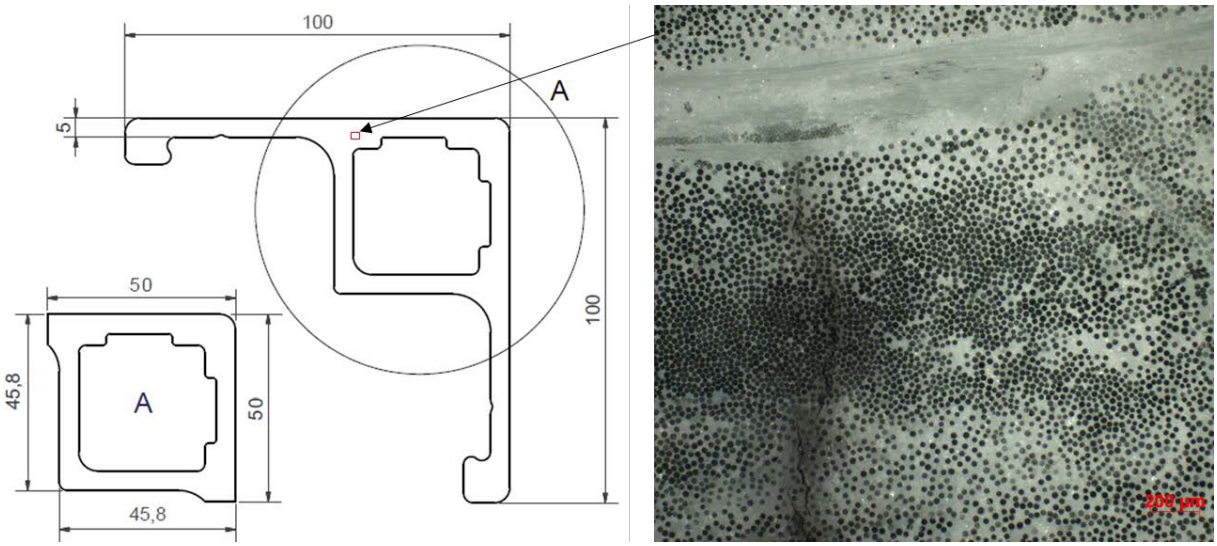

Fig.3: Definition of corner part and profile cross-section with picture of initial failure inside.

The profile was represented with 69 elements over the cross-section to fit the geometry reasonably well, and this mesh was extruded along the profile to represent the tested components with hex elements close to cubes geometrically. The idea illustrated in figure 4 was to allocate about 35 % of the cross-section area to elements representing fibres and the rest as matrix, and use reasonable material data for these two materials. The material model for the fibres was defined with density like 2620 kg/m^3, elastic modulus 69 GPa and true stress-strain curve following Voce law with A = 1200 MPa, Q_1 = 64.5 MPa, C_1 = 1000, Q_2 = 75 MPa, C_2 = 60 and Cockcroft-Latham value 15 MPa. Similar values for the matrix were density 1590 kg/m^3, E = 3.2 GPa, A = 30 MPa, Q_1 = 45 MPa, C_1 = 70, Q_2 = 50 MPa, C_2 = 1 and Wc = 1.0 MPa. This modelling approach seems to work well with ideal geometry as shown at left hand side in figure 4. However, moving some nodes to obtain some fibres not straight and moving some elements from the fibre part into the matrix part gives imperfect scaled fibres and matrix that reduces the predicted capacity by about 20 % in this case.

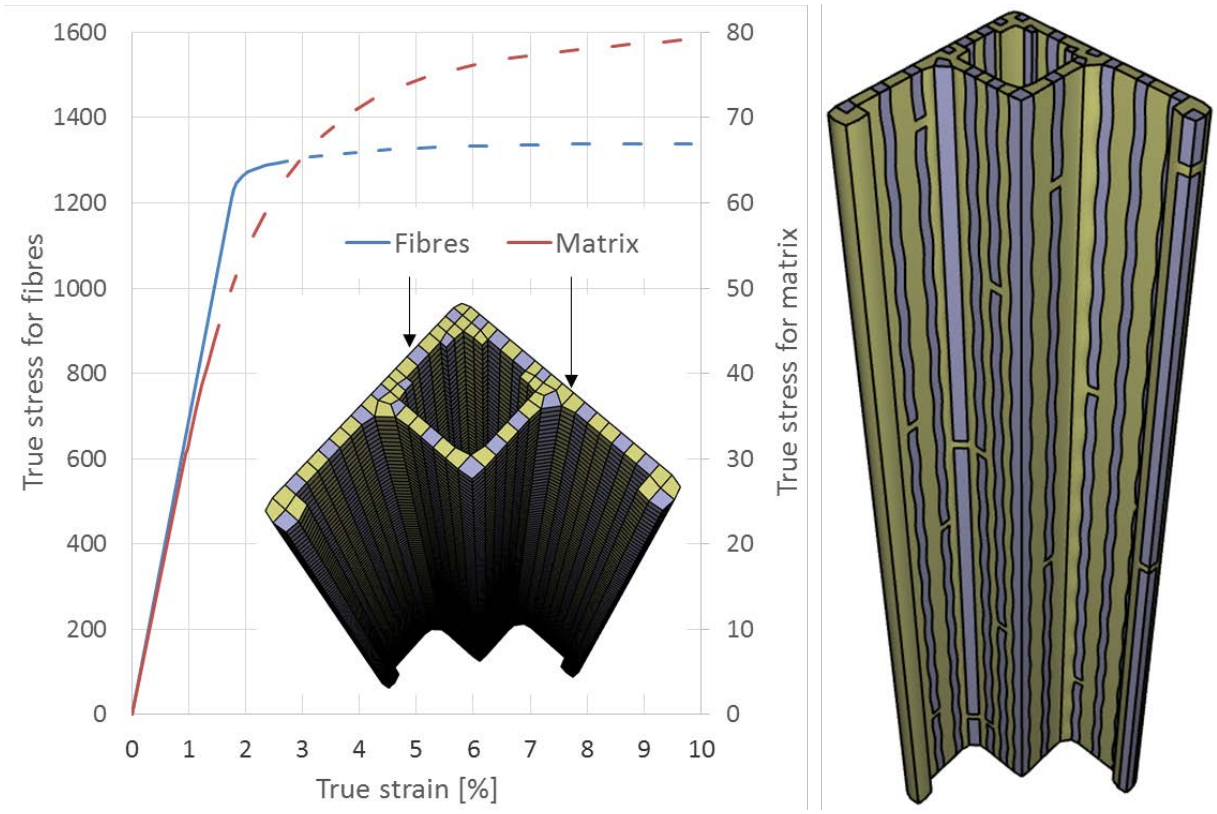

Fig.4: Modelling approach with realistic material curves for scaled fibres and matrix.

4 Comparison between test results and numerical predictions

The results from axial compression of the profile and the corner part are shown at left hand side in figure 5 for specimen lengths 240, 360 and 480 mm. The capacity is presented as maximum force divided by the cross-section area 1652 mm^2 for the profile and 1008 mm^2 for the corner part. The variation is relatively large for axial compression of the corner part only, and the cutting operation leaving two local areas along the specimen without surface layer and with free fibre ends may contribute to this scatter. An eventual tendency to increased capacity with increased specimen length is not significant, and the nine tests with axial compression of the corner part give 250 ± 38 kN. Mean value and standard deviation for the profile was 309 ± 20 kN, while 298 ± 5 kN indicates reduced variation and somewhat lower capacity for the longest profile. The force-displacement curves at right hand side in figure 5 shows that the corner part has lower axial stiffness than the profile where the free flanges contribute to the stiffness. However, it seems like the free flanges bend away and initiate collapse of the weakest part of the cross-section along the whole component length 480 mm. Local crushing at the weakest end limits the capacity for the corner parts, and even with length 480 mm this cross-section demonstrates sufficient stiffness to withstand global buckling. It is worth to notice that the strongest corner part demonstrates similar capacity as the profile.

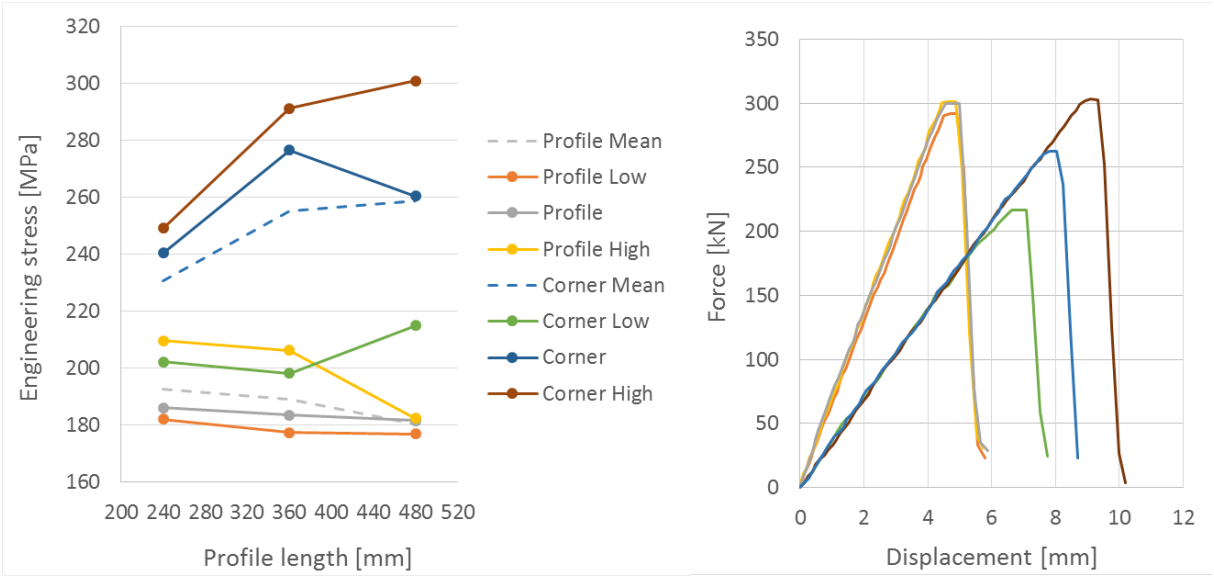

Fig.5: Capacity for profile and corner part as well as response curves for length 480 mm.

The free flanges does not have sufficient stiffness to contribute effectively to the capacity under axial compression, and this is often denoted as increased cross-section slenderness compared with the corner part that seems to represent a fully effective cross-section. Figure 6 shows a test arrangement with circular bars to secure low friction when measuring the stiffness transverse to the longitudinal fibres. Note that this test were run with two different profile lengths to compensate for the effect of free fibre ends.

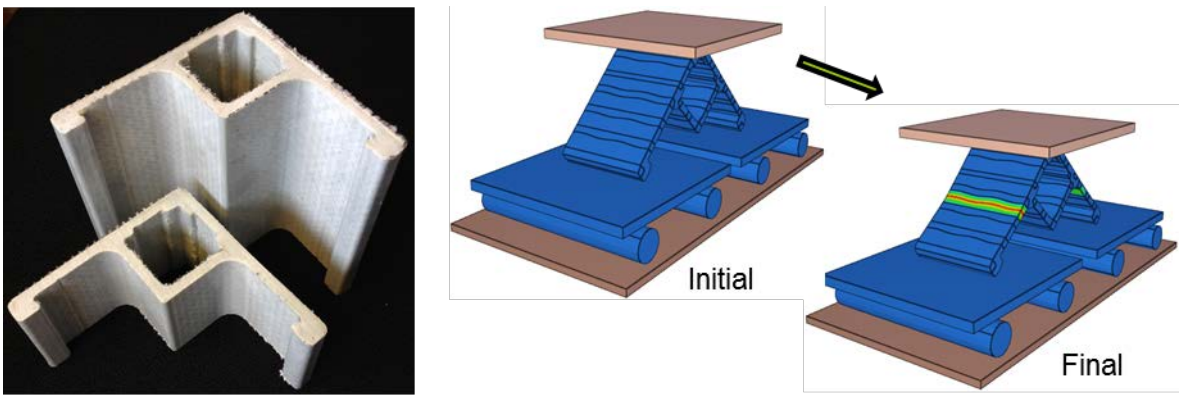

Fig.6: Test specimens with different length and FEM model of the test arrangement.

Figure 7 shows a comparison between numerical predictions and test results. It seems like this modelling approach with simple material models for fibre and matrix is able to predict the brittle behaviour. This means fracture initiated by the free flanges that bend away when testing the profile, crushing of the weakest end for axial compression of the not too long corner part only, and the deformation that localises into the weakest side in the test designed to measure the transverse stiffness.

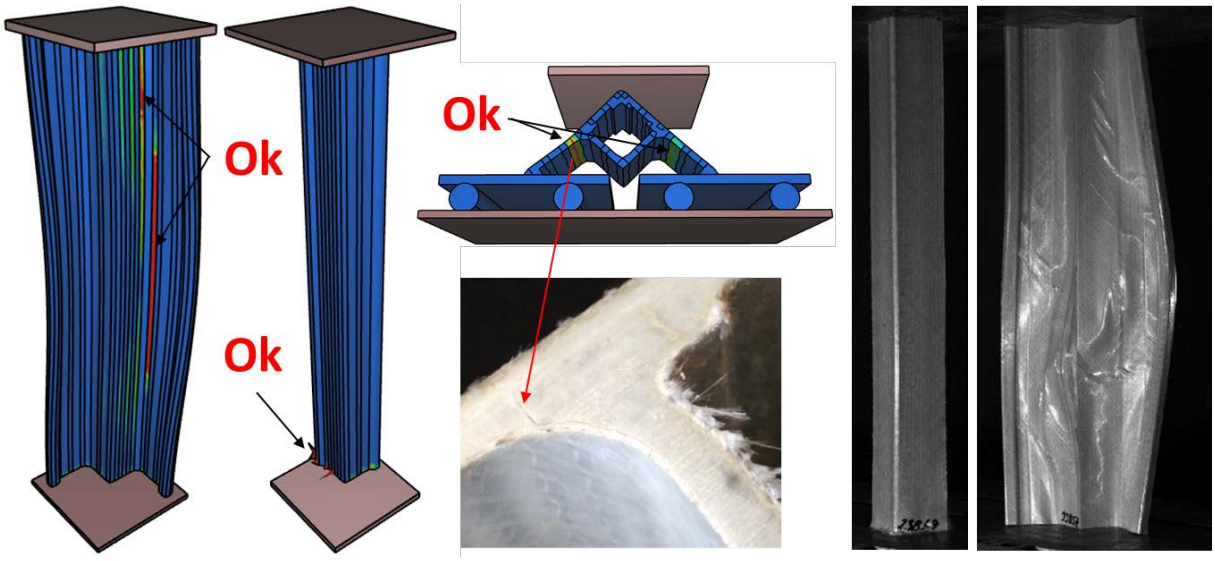

Fig.7: Experimental results and predicted deformation mode with scaled fibre and matrix.

5 An evaluation of this modelling approach for other profile geometries

Figure 8 shows three circular tubes with length 239 mm after tests with axial compression to measure the ultimate capacity. Note that one end was cut carefully to obtain one plane surface, while the original cut was kept at the other end. This means a curvature with two opposite amplitudes 0.4 mm above the lowest positions in between these two. It is likely that this shape at the end is the result of a plane cut beside some squeeze of the tube to support it during this operation. The high-speed video recording showed that the capacity was limited by local crushing from the curvature end for all of them. The tube shown in the middle with wall thickness measurements in the range 5.78 - 6.20 mm shows more regular crushing than the tube at left hand side in figure 8 with measured thickness values in the range like 5.67 - 6.33 mm. However, it is not possible to decide whether the non-regular behaviour was a result of initial defects in the tube or more thickness variation defined with coefficient of variation like 4.1 % compared with 2.4 % for the one with more regular crushing.

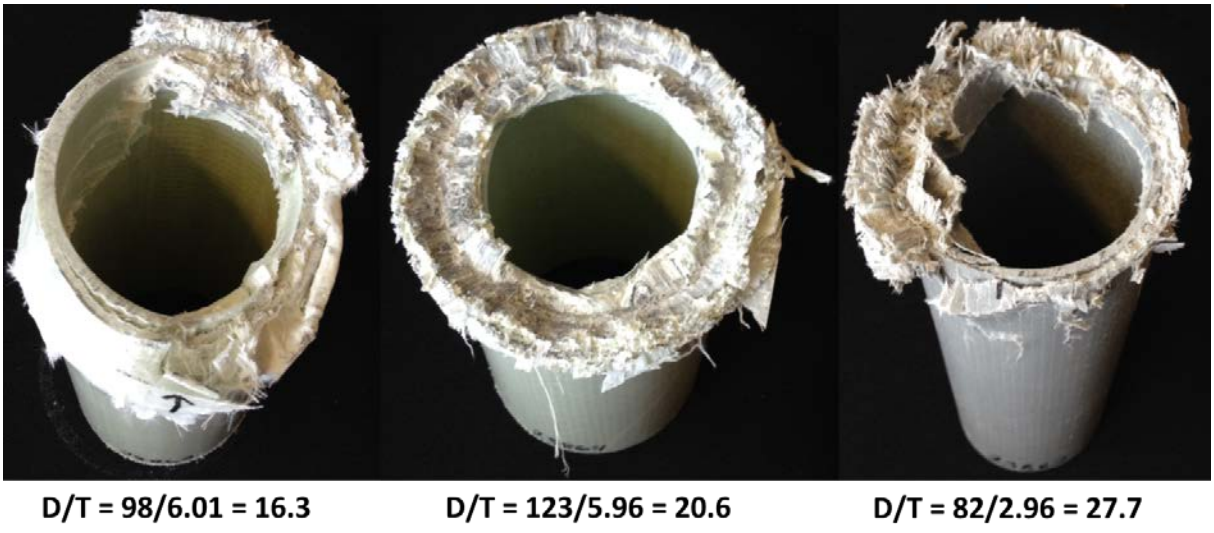

Fig.8: Axial compression of circular pultruded tubes with length 239 mm.

Also for the tube with highest cross-section slenderness and coefficient of thickness variation 3.5 % the capacity was limited by crushing from the curvature end. However as shown at right hand side in figure 8 there is some cracks some distance from the end that may indicate some initiation of 2-lobe buckling. The question is how large the diameter over thickness ratio has to be to before the capacity due to local buckling of the cross-section is lower than the capacity due to local crushing of the end. However, tubes with higher D/T-ratio than 27.7 were not available for testing to investigate this.

The transverse stiffness is important also for the circular pultruded tubes, and it was measured on the cross-section level by squeezing the profiles as illustrated in figure 9. The effect of fibres without anchoring at their free ends was assumed similar as for the profile with free flanges, and only one length like 40 mm was tested here. Two different mesh variants were used for the tube with lowest cross-section slenderness defined by D/T = 16.3, and it is worth to notice that both have 33 % of the area as longitudinal fibres as the five elements representing matrix around each fibre are somewhat smaller for the refined mesh. The predicted transverse stiffness was about the same for both variants, while the predicted capacity for the tube under axial compression was somewhat higher for the coarsest one. Both mesh variants have far too thick fibres compared with reality, but each fibre is covered by matrix where the shear stiffness is challenged to keep the fibres in position.

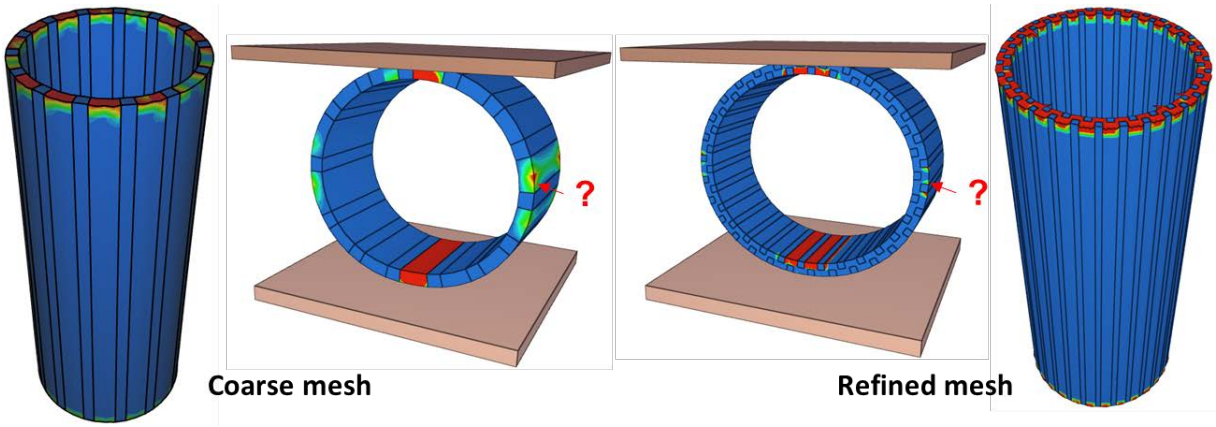

Fig.9: Two different mesh variants with scaled fibres and matrix for the tube with D/T=16.3

Figure 9 illustrates that this modelling approach seems able to predict crushing at the weakest end for these relatively short tubes under axial compression and collapse of the weakest position at three, six, nine or twelve o'clock when the tube is squeezed to measure transverse stiffness. However, the simulations were run with uniform wall thickness like the average value of the measurements, while the tubes with thickness variations in the ranges 2.81 - 3.08 mm and 5.67 - 6.33 mm showed cracks to the sides as well when the thinnest section was oriented at three or six o'clock. Remember that 10 % thickness variation means 33 % variation in bending stiffness for a uniform material. The positions of the fibres are important for composite materials, and the effect may be somewhat different here.

A comparison between the numerical predictions and the measurements of transverse stiffness indicates that the largest tube with diameter 123 mm and average thickness 5.96 mm had two times the transverse stiffness as assumed in the numerical model. It is likely that this tube is dimensioned for internal pressure and therefore has more fibres oriented along the circumference. Also the other two tubes had higher transverse stiffness than assumed, but the difference was not as large as for the tube shown in the middle in figure 8.

Figure 10 shows a comparison between the predicted response for these three circular tubes under axial compression and the experimental results. The correlation is far from perfect, but it seems reasonable compared with the variation we have to expect when testing composite parts like this.

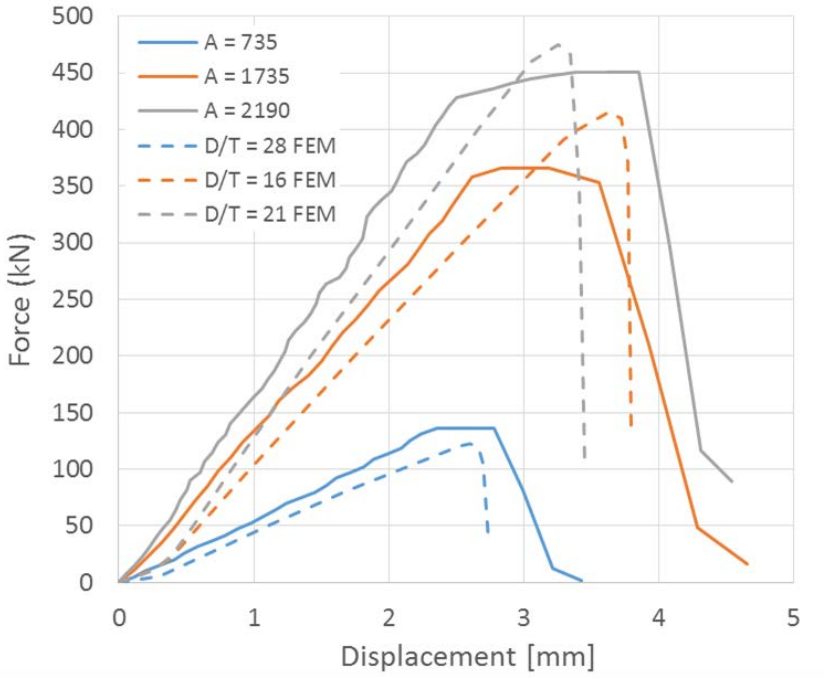

Fig.10: Comparison between numerical predictions and test results for the circular tubes.

6 Discussions and future work

The proposed modelling approach with realistic material properties for scaled fibres and matrix seems to give reasonable estimates also for other geometries than the profile used as base for this study. It is interesting to notice that the capacity is overestimated for the two tubes with the lowest cross-section slenderness, while it is underestimated for the most thin-walled one. Also the measurements that show higher transverse stiffness for the circular tubes than assumed here indicates an effect of more fibres in the other directions than along the profile compared to the base for this study. The proposed modelling approach aims to capture the axial stiffness with the share of the cross-section that is longitudinal fibres, while the only possible solution to capture higher transverse stiffness is to increase the matrix stiffness. The result is somewhat higher stiffness and capacity from the matrix unless higher transverse stiffness also means some reduced number of longitudinal fibres. However, an interesting possibility is to introduce initial mistakes as some elements moved from the fibre part into the matrix part. This is illustrated at left hand side of figure 11 where the displacement just before instability at the weakest end is scaled ten times. It is likely that the tendency to local buckling will decrease with higher transverse stiffness, and the predicted capacity will improve for a slender cross-section like this.

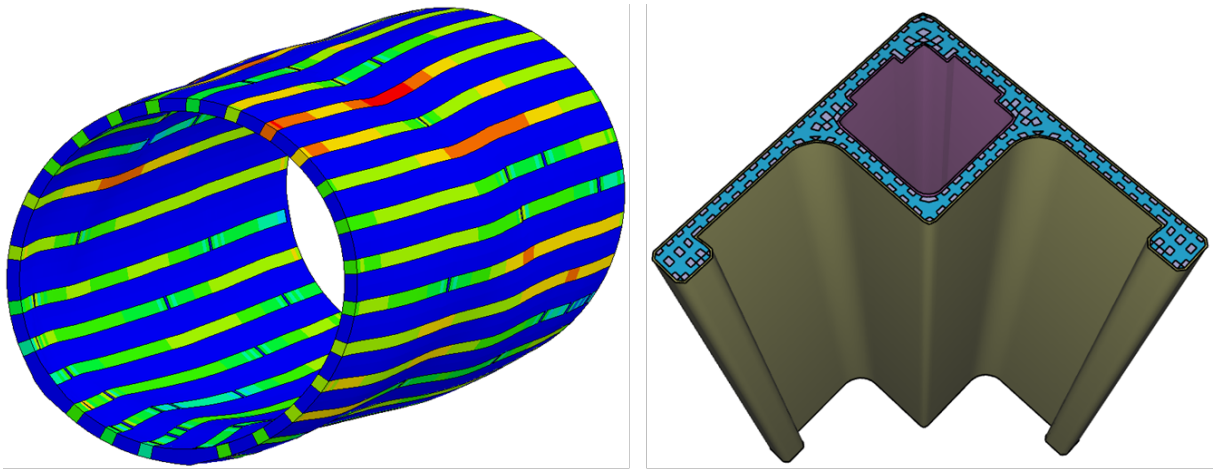

Effective stress and 10 times the displacement **Refined model of the base profile**

Fig.11: Some possibilities that may be investigated in the future.

It is also shown in figure 11 how a composite is far from a uniform material. The stain field may be more or less constant over the profile under axial compression, but the effective stress may be about 800 MPa in the fibres and about 40 MPa in the matrix. This is the result when combining materials with significant different stiffness and strength, and figure 4 illustrate this with different vertical axis for fibre and matrix. However, the connection between fibres and matrix is more critical with higher stress level, and initial mistakes mean discontinuities that challenge this connection even more. The idea here with common nodes is to avoid adding stiffness because of tied connections, and use a relatively low value for the Cockcroft-Latham parameter for the matrix material to remove this connection locally. The result of deleting the first element is a stress concentration that often lead to severe crack propagation, and the result of removing relatively large elements may be at least as dramatic and similar to the "explosion" captured by the high-speed camera during the experiments.

It is also worth to notice that the coarse mesh used in this modelling approach does not have possibilities for delamination between layers through the thickness like this was observed during the experiments. The surface layer keeps it together, but the cross-section stiffness is lost when the inner part of the cross-section is separated. It is likely that this behaviour can be captured by for example an orthogonal material model to represent the overall properties of the surface layer as a uniform part outside fibres and matrix inside the cross-section. This is illustrated with an example at right hand side in figure 11 where it may be challenge to allocate sufficiently many elements as fibres without common nodes between them.

Finally, it seems possible to make an even more realistic model of the composite profile in figure 4 where each of the 69 elements to define the cross-section are represented with something similar to the cubes at right hand side of figure 2. However, it will be a challenge to obtain a mesh quality that secure correct stiffness when modelling a complex geometry like this, and the computational time may be a challenge as well. It is therefore interesting to evaluate how complex and realistic the internal mix of fibres and matrix inside a component has to be represented to work sufficiently accurate as a design tool for composite parts. Here it is important to remember that the connections are often the most critical elements in many structures made of composite, and modelling of these should be included in an eventual study like this.

7 Summary

A composite profile was tested to evaluate global stiffness, cross-section stiffness and local matrix stiffness required to support the fibres under compression. The idea was to find a design tool for composite structures in the first stage where an estimate is useful to define a proper cross-section, and an engineering approach with realistic material properties and scaled fibres + matrix was developed.

8 Acknowledgements

The research within this study was supported by grant 260399/O20 from the Research Council of Norway. The support is gratefully acknowledged. Moreover, the support from Øglænd System and Impetus Afea made this research programme possible. Some features related to the composite profile in figures 1 and 3 are protected by Øglænd System.

9 Literature

[1] Tryland, T., Berstad, T.: "Keep the Material Model simple with input from Elements that predict the Correct Deformation Mode", 10th European LS-DYNA Conference, Würzburg, Germany, 2015.
[2] Tryland, T.: "Reduced Ductility due to Local Variation in Material Properties for 3D-printed Components", 11th European LS-DYNA Conference, Salzburg, Austria, 2017.
[3] Øglænd System.: "FRP Cable ladders, trays and support system", Product catalogue 07.12.